Transformation Theory for Spatiotemporal Metamaterials

Fubao Yang,[1,*] Liujun Xu,[2,†] Jun Wang[3,4] and Jiping Huang[1,‡]

[1]*Department of Physics, State Key Laboratory of Surface Physics, and Key Laboratory of Micro and Nano Photonic Structures (MOE), Fudan University, Shanghai 200438, China*

[2]*Graduate School of China Academy of Engineering Physics, Beijing 100193, China*

[3]*School of Physics, East China University of Science and Technology, Shanghai 200237, China*

[4]*Wenzhou Institute, University of Chinese Academy of Sciences, Wenzhou, China*

The transformation theory provides a distinct method for designing parameters in spatial dimensions, facilitating intriguing functions such as cloaking, concentrating, and rotating. However, with the introduction of temporal dimension, the transformation theory becomes particularly elusive because coordinate transformations apply only to static parameters. Here, we develop the transformation thermotics for designing spatiotemporal metamaterials. Specifically, we consider the transient heat-conduction equation with dynamic thermal parameters, whose transformation principles are theoretically derived and numerically confirmed. We further uncover spatiotemporal thermal cloaking, concentrating, and rotating with transformation thermotics as model applications. In contrast to conventional static parameters, dynamic parameters may provide unique opportunities for achieving thermal functions with the additional asymmetric feature. Our spatiotemporal scheme has remarkable advantages in dynamic heat regulation and provides insights into particle or plasma diffusion and wave propagation.

I. INTRODUCTION

The temporal dimension has opened an exotic gate for metamaterial design [1,2]. In contrast to conventional metamaterials, spatiotemporal metamaterials facilitate unique properties and functions, such as time-inversion symmetry breaking [3,4], Floquet topological insulators [5,6], and digital coding metasurfaces [7–9]. Besides wave systems, the temporal dimension has also received intensive attraction in diffusive systems, yielding asymmetric diffusion [10–15] and topological transport [16–18]. Nevertheless, a universal theory for designing dynamic parameters is still lacking, making the temporal dimension extremely difficult to control.

On the other hand, the transformation theory provides a fundamental method for designing metamaterials at will [19,20]. Originating from transformation optics [21], transformation thermotics [22–25] has become an indispensable tool for designing thermal metamaterials [26,27]. Compared with the original version [22], transformation thermotics has been able to deal with anisotropic and nonlinear thermal conductivities [23,28,29], transient heat conduction [30,31], dynamics coordinate transformations [32], and multiphysical field coupling [33–42]. However,

a severe limitation is that transformation thermotics still cannot handle dynamic thermal parameters, largely limiting practical applications. With the temporal dimension becoming increasingly crucial [1,2], it is urgent to develop the transformation theory for designing dynamic thermal parameters.

To solve this pressing problem, we develop the transformation theory for designing spatiotemporal metamaterials, thereby providing a promising degree of freedom for the metamaterial design. Taking heat transfer as an example, we consider the transient thermal conduction equation (based on the Fourier law) with dynamic thermal parameters [Figs. 1(a) and 1(b)]. Specifically, material *B* (homogeneous background) with static thermal parameters [Fig. 1(a)] is converted into material *A* [Fig. 1(b)] by an external field [10]. Thus, we obtain a material with dynamic thermal parameters by driving the external field to move. We theoretically derive the transformation principles of these dynamic thermal parameters, thereby developing the transformation thermotics for spatiotemporal metamaterials. For practical applications, we consider wavelike spatiotemporal modulation and design three typical functions with spatiotemporal transformation metamaterials, i.e., thermal cloaking, concentrating, and rotating [Figs. 1(c)–1(e)]. The proposed method bridges the transformation theory and the temporal dimension, delivering opportunities in dynamic heat regulation. Besides, our results inspire the dynamic control of nonthermal

fields, such as particle or plasma diffusion and wave propagation.

II. TRANSFORMATION THERMOTICS FOR SPATIOTEMPORAL METAMATERIALS

The Fourier law governs the transient heat conduction in macroscopic solids, whose energy conservation equation is [14]

$$\frac{\partial (\rho c T)}{\partial t} + \nabla \cdot (-\kappa \nabla T) = Q, \tag{1}$$

where ρ, c, and κ are the mass density, heat capacity, and thermal conductivity of the material, respectively. T denotes temperature, t is time, and Q is heat power density. In contrast to conventional transformation thermotics [22,23,28,30,31], we suppose these thermal parameters to be dynamic, indicating that the material properties are modulated spatiotemporally. Then, the governing equation of heat transfer becomes

$$\frac{\partial (\rho (r,t) c (r,t) T)}{\partial t} + \nabla \cdot (-\kappa (r,t) \nabla T) = Q (r,t), \tag{2}$$

where the parameters vary in time and space. Restricted by mass conservation, the spatiotemporal modulation of mass density inevitably produces a local mass flow [14], thus affecting heat transfer. To avoid this influence, mass density is set as a constant, and only heat capacity and thermal conductivity are modulated in space and time. Thus, the heat-conduction equation is reduced to

$$\frac{\partial (C (r,t) T)}{\partial t} + \nabla \cdot (-\kappa (r,t) \nabla T) = Q (r,t), \tag{3}$$

where $C(r,t)$ is the product of heat capacity and constant mass density.

The heat-conduction equation described by Eq. (3) is universal in different spaces. We consider a curvilinear space **S** with contravariant coordinates $\{x^1, x^2, x^3\}$, contravariant basis $\{\mathbf{g}^1, \mathbf{g}^2, \mathbf{g}^3\}$, and covariant basis $\{\mathbf{g}_1, \mathbf{g}_2, \mathbf{g}_3\}$. Therefore, $\nabla \cdot (\kappa (r,t) \nabla T)$ in Eq. (3) becomes

$$\nabla \cdot (\kappa (r,t) \nabla T) = \mathbf{g}^k \cdot \frac{\partial}{\partial x^k} \left(\kappa^{ij} (r,t) \mathbf{g}_i \otimes \mathbf{g}_j \cdot \mathbf{g}^l \frac{\partial T}{\partial x^l} \right)$$

$$= \mathbf{g}^k \cdot \frac{\partial}{\partial x^k} \left(\kappa^{ij} (r,t) \mathbf{g}_i \frac{\partial T}{\partial x^j} \right)$$

$$= \frac{\partial}{\partial x^i} \left(\kappa^{ij} (r,t) \frac{\partial T}{\partial x^j} \right)$$

$$+ \mathbf{g}^k \cdot \frac{\partial \mathbf{g}_i}{\partial x^k} \left(\kappa^{ij} (r,t) \frac{\partial T}{\partial x^j} \right)$$

$$= \frac{\partial}{\partial x^i} \left(\kappa^{ij} (r,t) \frac{\partial T}{\partial x^j} \right)$$

$$+ \Gamma_{ki}^k \left(\kappa^{ij} (r,t) \frac{\partial T}{\partial x^j} \right)$$

$$= \frac{1}{\sqrt{g}} \partial_i \left(\sqrt{g} \kappa^{ij} (r,t) \partial_j T \right), \tag{4}$$

where i, j, k, l take $1, 2, 3$. The Christoffel symbol is defined as $\Gamma_{jk}^i = (\partial \mathbf{g}_k / \partial x^j) \cdot \mathbf{g}^i$ and satisfies $\Gamma_{ki}^k = (\partial_i \sqrt{g}) / \sqrt{g}$, where g is the determinant of the matrix with the component of $g_{ij} = \mathbf{g}_i \cdot \mathbf{g}_j$. Substituting Eq. (4) into Eq. (3), we have

$$\partial_t \left(\sqrt{g} C (r,t) T \right) + \partial_i \left(-\sqrt{g} \kappa^{ij} (r,t) \partial_j T \right) = \sqrt{g} Q (r,t). \tag{5}$$

To realize the same effect in the physical space, we rewrite Eq. (5) in the physical space with contravariant coordinates $\{x^{1'}, x^{2'}, x^{3'}\}$,

$$\partial_t \left(\sqrt{g} C (r,t) T \right) + \partial_{i'} \left(-\sqrt{g} J_i^{i'} \kappa^{ij} (r,t) J_j^{j'} \partial_{j'} T \right)$$

$$= \sqrt{g} Q (r,t), \tag{6}$$

where **J** is the Jacobian transformation matrix describing the transformation from the curvilinear to physical spaces, $J_i^{i'} = \partial x^{i'} / \partial x^i$ is the component of **J**, and $\sqrt{g} = \det^{-1} \mathbf{J}$. Considering the heat-conduction equation in the physical space, i.e., $\partial_t \left(C' (r',t) T \right) + \partial_{i'} \left(-\kappa^{i'j'} (r',t) \partial_{j'} T \right) = Q' (r',t)$, we derive the transformed parameters in the physical space,

$$C' (r',t) = \frac{C (r,t)}{\det \mathbf{J}}, \tag{7a}$$

$$\kappa' (r',t) = \frac{\mathbf{J} \kappa (r,t) \mathbf{J}^{\dagger}}{\det \mathbf{J}}, \tag{7b}$$

$$Q' (r',t) = \frac{Q (r,t)}{\det \mathbf{J}}, \tag{7c}$$

where $C (r,t)$ can also be treated as the product of heat capacity and mass density of the background [region III in Fig. 1(b)], and $\kappa (r,t)$ is its thermal conductivity. Note that r should be expressed by r' for preciseness, and $\mathbf{J}^{\dagger}$ denotes the transpose of **J**. $C' (r',t)$ and $\kappa' (r',t)$ are the parameters of the transformed regions I and II. Therefore, Eq. (7) provides a universal method for designing dynamic thermal parameters.
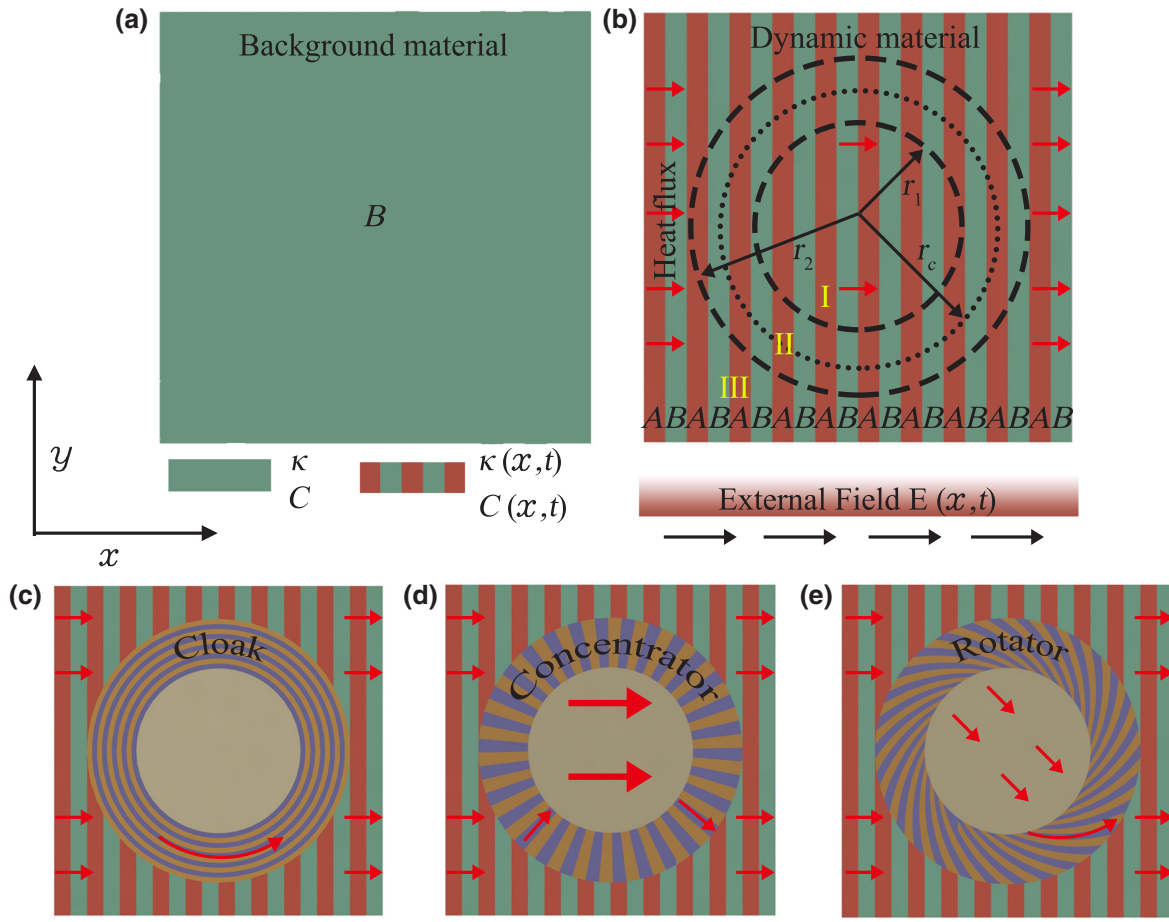
FIG. 1. Schematic diagrams of spatiotemporal metamaterials. (a) Homogeneous background with constant thermal conductivity and product of heat capacity and mass density. (b) Dynamic material with thermal conductivity and product of heat capacity and mass density modulated by an external field moving along the x direction. Regions I, II, and III denote the core, shell, and background. The arrows represent heat flux. (c) Illustration of a thermal cloak. The heat flux bypasses the center, and infrared detection cannot find the central objects. (d) Schematic of a thermal concentrator. The heat flux increases inside the concentrator. (e) Illustration of a thermal rotator. The heat flux changes its direction in the core.

III. SPATIOTEMPORAL THERMAL FUNCTIONS

Equation (7) is the key to spatiotemporal transformation thermotics. As shown in Figs. 1(c)–1(e), we design three typical thermal metamaterials with two-dimensional cylindrical coordinates (r and θ), i.e., cloaking, concentrating, and rotating.

A thermal cloak prevents heat flow into the central region. For this purpose, a circular region ($r < r_2$) is compressed into a shell region ($r_1 < r < r_2$), and its transformation is

$$r' = (r_2 - r_1)r/r_2 + r_1, \quad (r < r_2), \tag{8a}$$

$$\theta' = \theta, \tag{8b}$$

where r_1 and r_2 are the inner and outer radii, respectively.

A thermal concentrator gathers heat flow and increases the temperature gradient in the central region. So the space

transformation is to squeeze a larger circular region $r < r_c$ into a small one $r < r_1$ and stretch the shell region $r_c < r < r_2$ into the shell region $r_1 < r < r_2$. The transformation can be expressed as

$$r' = r_1 r/r_c, \quad (r < r_c), \tag{9a}$$

$$r' = ((r_2 - r_1) r + (r_1 - r_c) r_2) / \\ \times (r_2 - r_c), \quad (r_c < r < r_2), \tag{9b}$$

$$\theta' = \theta, \tag{9c}$$

where r_c determines the concentrating degree of the central temperature gradient, with a maximum value of r_2.

A thermal rotator changes the direction of heat flow in the central region. To this end, the core region $r < r_1$ is rotated by an angle of θ_0, and in the shell region $r_1 < r < r_2$, the rotation angle gradually increases from zero to θ_0 as
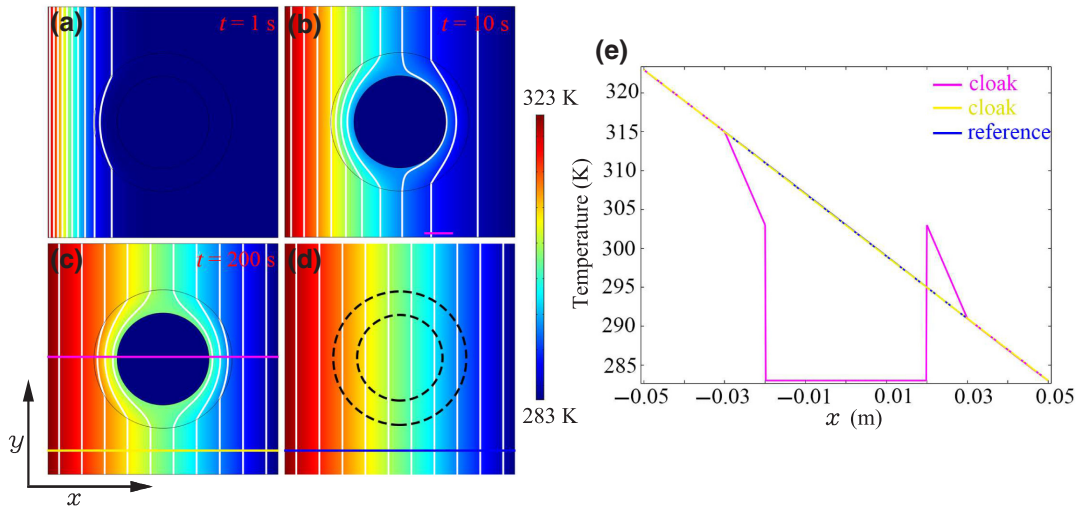
FIG. 2. Simulations of spatiotemporal thermal cloaking. The rainbow colors denote temperatures, and the white lines are isotherms. The parameters of the original dynamic material are $\kappa_a = 100$ W m^{-1} K^{-1}, $\kappa_b = 300$ W m^{-1} K^{-1}, $C_a = 5 \times 10^5$ J m^{-3} K^{-1}, $C_b = 3 \times 10^6$ J m^{-3} K^{-1}, $k = 50$ m^{-1}, $\omega = 25$ s^{-1}. (a)–(c) Temperature distributions at $t = 1$ s, $t = 10$ s, and $t = 200$ s, respectively. (d) Temperature distribution of an untransformed dynamic material, serving as a reference. (e) Temperatures extracted from three marked lines.

r decreases. Its transformation can be written as

$$r' = r, \tag{10a}$$

$$\theta' = \theta + \theta_0, \ (r < r_1), \tag{10b}$$

$$\theta' = \theta + \theta_0(r_2 - r)/(r_2 - r_1), \ (r_1 < r < r_2), \tag{10c}$$

where θ_0 is the rotation angle.

The corresponding Jacobian transformation matrix with two-dimensional cylindrical coordinates is calculated by

$$\mathbf{J} = \begin{pmatrix} \partial r'/\partial r & \partial r'/(r\partial\theta) \\ r'\partial\theta'/\partial r & r'\partial\theta'/(r\partial\theta) \end{pmatrix}. \tag{11}$$

Substituting Eqs. (8)–(11) into the transformation principles described by Eq. (7), we finally derive the dynamic thermal parameters in the transformed regions I and II. Since the original parameters are spatiotemporally modulated and expressed in terms of r rather than r', we should rewrite the parameters obtained from Eq. (7) in the transformed coordinate system. We take spatiotemporal thermal cloaking as an example and consider the wavelike spatiotemporal modulation for brevity [10–13]. The dynamic thermal conductivity of the original material in region II is $\kappa_0(x,t) = \kappa_a \cos(kx - \omega t) + \kappa_b$, where κ_a is the variation amplitude, κ_b is the balanced thermal conductivity, k is the modulation wave number, and ω is the modulation angular frequency. The transformed thermal conductivity is $\kappa'(x',t) = \mathbf{J}(\kappa_a \cos(kx - \omega t) + \kappa_b)\mathbf{J}^\dagger/\det\mathbf{J}$. We should express x in terms of x' in the transformed coordinate system,

$$\frac{x}{x'} = \frac{r\cos\theta}{r'\cos\theta'}. \tag{12}$$

According to Eq. (8), we have

$$\frac{x}{x'} = \frac{r\cos\theta}{r'\cos\theta'} = \frac{(r' - r_1)r_2}{(r_2 - r_1)r'}. \tag{13}$$

Therefore, the final expression of the transformed thermal conductivity for cloaking is $\kappa'(x',t) = \mathbf{J}(\kappa_a \cos(kx'(r' - r_1)r_2/((r_2 - r_1)r') - \omega t) + \kappa_b)\mathbf{J}^\dagger/\det\mathbf{J}$. For thermal concentrating and rotating, we calculate the transformed thermal parameters in a similar way.

IV. FINITE-ELEMENT SIMULATIONS

We perform transient finite-element simulations with COMSOL Multiphysics in the two-dimensional heat-transfer module in solids to validate the transformation theory for designing spatiotemporal metamaterials. Due to the limitation of finite-element simulations, the governing equation is in the form of Eq. (14). To match the theory to the simulation, we set $Q(r,t) = T\partial_t C(r,t)$ in Eq. (3). Finally, the governing equation is reduced to [10–13]

$$C(r,t)\frac{\partial T}{\partial t} + \nabla \cdot (-\kappa(r,t)\nabla T) = 0. \tag{14}$$

This simplification does not affect our main results described by Eq. (7). These three spatiotemporal thermal metamaterials have core-shell structures. They have the
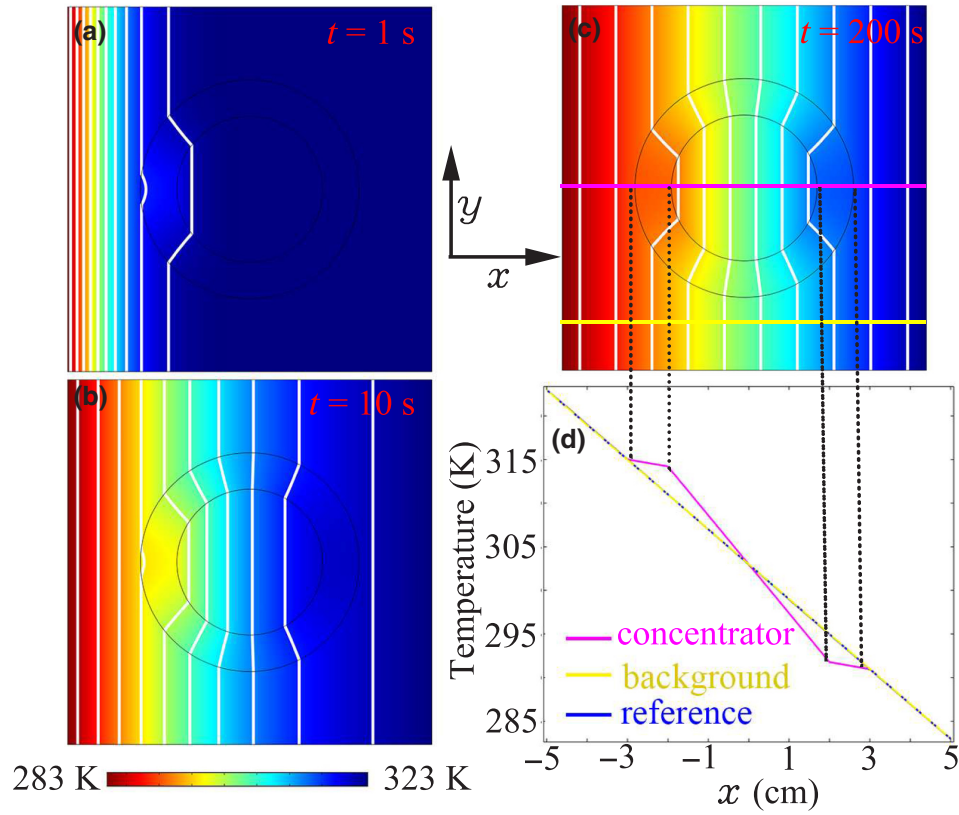
FIG. 3. Simulations of spatiotemporal thermal concentrating. All parameters are unchanged except for regions I and II, which are calculated according to Eqs. (7) and (9).

same sizes and parameters except for regions I and II, as shown in Fig. 1. The square model length is $a = 10$ cm. The inner and outer radii are $r_1 = 2$ cm and $r_2 = 3$ cm, respectively. Before the transformation, the background material is spatiotemporally modulated with dynamic thermal parameters of $\kappa_0 = \kappa_a \cos(kx - \omega t) + \kappa_b$ and $C_0 = C_a \cos(kx - \omega t) + C_b$. We set the initial temperature at 283 K. The left and right sides are hot and cold sources with temperatures of 323 and 283 K. The transient simulation takes about 200 s to reach the steady state, and we demonstrate the simulation effect at 1, 10, and 200 s. The transient finite-element simulations of three thermal metamaterials are shown in Figs. 2–4.

The parameters of thermal cloaking are derived according to Eqs. (7) and (8). Figures 2(a)–2(c) show the temperature profiles evolving to the steady state. Heat fluxes do not flow into the central region I, and the background temperature profile is not distorted, indicating that the spatiotemporal thermal cloak works well. To confirm our theory more accurately, we extract the temperature data on the pink and yellow lines in Fig. 2(c) and compare them with the reference temperature data extracted from the untransformed background material [the blue line in Fig. 2(d)]. Figure 2(e) is the comparison diagram. The cloaking temperature is consistent with the reference except for regions

I and II. Besides, the temperature gradient is zero in region I, indicating the excellent cloaking performance.

The concentrating parameters are calculated from Eqs. (7) and (9). Figures 3(a)–3(c) show the temperature evolutions of the thermal concentrator reaching the steady state. The background temperature profile is not distorted, and the isotherms in region I are concentrated. Since the background materials of our thermal metamaterials are the same, Fig. 2(d) is also applicable to thermal concentrating and rotating as a reference. Comparing the temperature data extracted from the pink and yellow lines in Fig. 3(c) with the reference line, we observe that the temperature distribution of the thermal concentrator is consistent with that of the reference in region III. Meanwhile, the temperature gradient in region I increases, as shown in Fig. 3(d). These results validate the concentrating effect.

The parameters of spatiotemporal thermal rotating are calculated from Eqs. (7) and (10), with a rotation angle of $\theta_0 = \pi$. Similarly, Figs. 4(a)–4(c) show the temperature profiles of the thermal rotator, and Fig. 4(d) shows the comparison between the temperature data extracted from the pink and yellow lines in Fig. 4(c) and the reference line. The heat flux direction in region I is reversed 180°, and the rotating effect is also excellent.
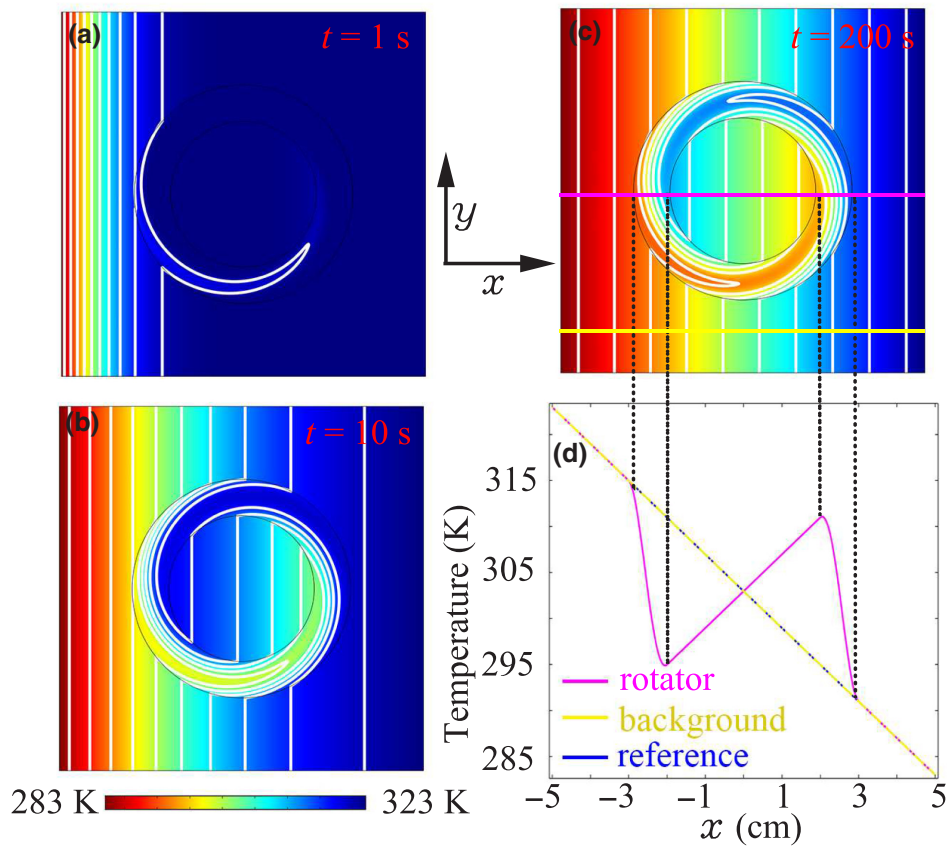
FIG. 4.   Simulations of spatiotemporal thermal rotating. All parameters are unchanged except for regions I and II, which are calculated according to Eqs. (7) and (10).

To make the transformation theory for spatiotemporal metamaterials more intuitive, we show the time-dependent material parameters and temperature distributions in Sec. I within the Supplemental Material as GIF files [56]. The animations change too fast because the period of the thermal parameters is much smaller than the time for the thermal system to reach a steady state. To observe the change of the time-dependent thermal parameters and temperature distribution more clearly, we provide animations for several periods after the system reaches the steady state, see Sec. II within the Supplemental Material [56]. The temperature distributions do not change significantly because the thermal diffusivity is large, so the system cannot respond to the rapidly evolving thermal parameters in real time. Moreover, we also conduct simulations in the electric charge diffusion field to prove that the idea can be extended to other physical fields, see Sec. III within the Supplemental Material [56].

V. DISCUSSION AND CONCLUSION

Besides thermal conductivity, we choose heat capacity as another dynamic parameter rather than mass density because the spatiotemporal modulation of mass density produces a mass flow that affects the form of Eq. (14). This

effect is critical to whether a heat-transfer process is reciprocal [10,11,14]. Nevertheless, we mainly care about the validity of the spatiotemporal transformation theory, and considering heat capacity or mass density has no essential difference, thus not affecting our conclusions. Note that heat transfer in this work could be nonreciprocal because Eq. (14) with appropriate parameter setting leads to asymmetry [10]. Nevertheless, for clarity, the parameters we choose are in the symmetric limit, so the simulation results indicate that heat transfer is symmetric. Fortunately, the temporal dimension still provides a distinct opportunity to achieve thermal asymmetry by the Willis coupling mechanism [15]. For experimental demonstration, we may construct a rotatable structure to achieve the spatiotemporal modulation of thermal parameters [11,43,44]. Moreover, many studies suggest that thermal conductivity and heat capacity can be regulated by external fields, such as electric fields [45,46] and light fields [47]. Therefore, we can realize spatiotemporal transformation metamaterials by applying appropriate external fields to target regions.

Furthermore, the proposed transformation theory for designing spatiotemporal metamaterials is not limited to thermal diffusion systems and can be extended to other physical fields, including particle or plasma diffusion

[48–52], wave propagation [1,2], and even multiphysics [35–42,53]. The introduction of the temporal dimension does not affect the form invariance of the governing equation under coordinate transformations. Therefore, we can design spatiotemporal transformation metamaterials in a similar way that we design conventional transformation metamaterials [19,20].

In conclusion, we develop the transformation theory and propose the concept of spatiotemporal transformation metamaterials. To verify the proposed theory, we take thermal conduction as an example and design three spatiotemporal thermal metamaterials with cloaking, concentrating, and rotating functions. The simulated results demonstrate the robustness of the proposed theory. The present work provides a fundamental method to design dynamic parameters and promote the applications of spatiotemporal metamaterials in diodes and beyond [54,55].

ACKNOWLEDGMENTS

[1] S. X. Yin, E. Galiffi, and A. Alù, Floquet metamaterials, eLight **2**, 8 (2022).

[2] L. Q. Yuan and S. H. Fan, Temporal modulation brings metamaterials into new era, Light: Sci. Appl. **11**, 173 (2022).

[3] D. L. Sounas and A. Alù, Non-reciprocal photonics based on time modulation, Nat. Photonics **11**, 774 (2017).

[4] H. Nassar, B. Yousefzadeh, R. Fleury, M. Ruzzene, A. Alù, C. Daraio, A. N. Norris, G. L. Huang, and M. R. Haberman, Nonreciprocity in acoustic and elastic materials, Nat. Rev. Mater. **5**, 667 (2020).

[5] M. S. Rudner and N. H. Lindner, Band structure engineering and non-equilibrium dynamics in Floquet topological insulators, Nat. Rev. Phys. **2**, 229 (2020).

[6] F. Zangeneh-Nejad, A. Alù, and R. Fleury, Topological wave insulators: A review, C. R. Phys. **21**, 467 (2020).

[7] L. Zhang, X. Q. Chen, S. Liu, Q. Zhang, J. Zhao, J. Y. Dai, G. D. Bai, X. Wan, Q. Cheng, G. Castaldi, V. Galdi, and T. J. Cui, Space-time-coding digital metasurfaces, Nat. Commun. **9**, 4334 (2018).

[8] C. Liu, Q. Ma, Z. J. Luo, Q. R. Hong, Q. Xiao, H. C. Zhang, L. Miao, W. M. Yu, Q. Cheng, L. L. Li, and T. J. Cui, A programmable diffractive deep neural network based on a digital-coding metasurface array, Nat. Electron. **5**, 113 (2022).

[9] M. Z. Chen, W. K. Tang, J. Y. Dai, J. C. Ke, L. Zhang, C. Zhang, J. Yang, L. L. Li, Q. Cheng, S. Jin, and T. J. Cui, Accurate and broadband manipulations of harmonic amplitudes and phases to reach 256 QAM millimeter-wave wireless communications by time-domain digital coding metasurface, Natl. Sci. Rev. **9**, nwab134 (2022).

[10] D. Torrent, O. Poncelet, and J. C. Batsale, Nonreciprocal Thermal Material by Spatiotemporal Modulation, Phys. Rev. Lett. **120**, 125501 (2018).

[11] M. Camacho, B. Edwards, and N. Engheta, Achieving asymmetry and trapping in diffusion with spatiotemporal metamaterials, Nat. Commun. **11**, 3733 (2020).

[12] L. J. Xu, J. P. Huang, and X. P. Ouyang, Tunable thermal wave nonreciprocity by spatiotemporal modulation, Phys. Rev. E **103**, 032128 (2021).

[13] J. Ordonez-Miranda, Y. Y. Guo, J. J. Alvarado-Gil, S. Volz, and M. Nomura, Thermal-Wave Diode, Phys. Rev. Appl. **16**, L041002 (2021).

[14] J. X. Li, Y. Li, P. C. Cao, M. H. Qi, X. Zheng, Y. G. Peng, B. W. Li, X. F. Zhu, A. Alù, H. S. Chen, and C.-W. Qiu, Reciprocity of thermal diffusion in time-modulated systems, Nat. Commun. **13**, 167 (2022).

[15] L. J. Xu, G. Q. Xu, J. P. Huang, and C.-W. Qiu, Diffusive Fizeau Drag in Spatiotemporal Thermal Metamaterials, Phys. Rev. Lett. **128**, 145901 (2022).

[16] G. Q. Xu, Y. H. Yang, X. Zhou, H. S. Chen, A. Alù, and C.-W. Qiu, Diffusive topological transport in spatiotemporal thermal lattices, Nat. Phys. **18**, 450 (2022).

[17] H. Hu, S. Han, Y. H. Yang, D. J. Liu, H. R. Xue, G.-G. Liu, Z. Y. Cheng, Q. J. Wang, S. Zhang, B. L. Zhang, and Y. Luo, Observation of topological edge states in thermal diffusion, Adv. Mater. **34**, 2202257 (2022).

[18] M. H. Qi, D. Wang, P.-C. Cao, X.-F. Zhu, C.-W. Qiu, H. S. Chen, and Y. Li, Geometric phase and localized heat diffusion, Adv. Mater. **34**, 2202241 (2022).

[19] L. Xu and H. Y. Chen, Conformal transformation optics, Nat. Photonics **9**, 15 (2015).

[20] L. Xu and H. Chen, Transformation metamaterials, Adv. Mater. **33**, 2005489 (2021).

[21] J. B. Pendry, D. Schurig, and D. R. Smith, Controlling electromagnetic fields, Science **312**, 1780 (2006).

[22] C. Z. Fan, Y. Gao, and J. P. Huang, Shaped graded materials with an apparent negative thermal conductivity, Appl. Phys. Lett. **92**, 251907 (2008).

[23] T. Y. Chen, C.-N. Weng, and J.-S. Chen, Cloak for curvilinearly anisotropic media in conduction, Appl. Phys. Lett. **93**, 114103 (2008).

[24] J.-P. Huang, *Theoretical Thermotics: Transformation Thermotics and Extended Theories for Thermal Metamaterials* (Springer, Singapore, 2020).

[25] L.-J. Xu and J.-P. Huang, *Transformation Thermotics and Extended Theories: Inside and Outside Metamaterials* (Springer, Singapore, 2022).

[26] S. Yang, J. Wang, G. L. Dai, F. B. Yang, and J. P. Huang, Controlling macroscopic heat transfer with thermal metamaterials: Theory, experiment and application, Phys. Rep. **908**, 1 (2021).

[27] Y. Li, W. Li, T. C. Han, X. Zheng, J. X. Li, B. W. Li, S. H. Fan, and C.-W. Qiu, Transforming heat transfer with thermal metamaterials and devices, Nat. Rev. Mater. **6**, 488 (2021).

[28] Y. Li, X. Y. Shen, Z. H. Wu, J. Y. Huang, Y. X. Chen, Y. S. Ni, and J. P. Huang, Temperature-Dependent Transformation Thermotics: From Switchable Thermal Cloaks to Macroscopic Thermal Diodes, Phys. Rev. Lett. **115**, 195503 (2015).

[29] F. B. Yang, B. Y. Tian, L. J. Xu, and J. P. Huang, Experimental Demonstration of Thermal Chameleonlike Rotators with Transformation-Invariant Metamaterials, Phys. Rev. Appl. **14,** 054024 (2020).

[30] S. Guenneau, C. Amra, and D. Veynante, Transformation thermodynamics: Cloaking and concentrating heat flux, Opt. Express **20,** 8207 (2012).

[31] R. Schittny, M. Kadic, S. Guenneau, and M. Wegener, Experiments on Transformation Thermodynamics: Molding the Flow of Heat, Phys. Rev. Lett. **110,** 195901 (2013).

[32] C. García-Meca and C. Barceló, Dynamically tunable transformation thermodynamics, J. Opt. **18,** 044026 (2016).

[33] J. Y. Li, Y. Gao, and J. P. Huang, A bifunctional cloak using transformation media, J. Appl. Phys. **108,** 074504 (2010).

[34] Y. G. Ma, Y. C. Liu, M. Raza, Y. D. Wang, and S. L. He, Experimental Demonstration of a Multiphysics Cloak: Manipulating Heat Flux and Electric Current Simultaneously, Phys. Rev. Lett. **113,** 205501 (2014).

[35] T. Stedman and L. M. Woods, Cloaking of thermoelectric transport, Sci. Rep. **7,** 6988 (2017).

[36] L. J. Xu, G. L. Dai, and J. P. Huang, Transformation Multithermotics: Controlling Radiation and Conduction Simultaneously, Phys. Rev. Appl. **13,** 024063 (2020).

[37] L. J. Xu and J. P. Huang, Negative thermal transport in conduction and advection, Chin. Phys. Lett **37,** 080502 (2020).

[38] L. J. Xu and J. P. Huang, Active thermal wave cloak, Chin. Phys. Lett **37,** 120501 (2020).

[39] L. J. Xu, S. Yang, and J. P. Huang, Controlling thermal waves of conduction and convection, EPL **133,** 20006 (2021).

[40] W.-S. Yeung, V.-P. Mai, and R.-J. Yang, Cloaking: Controlling Thermal and Hydrodynamic Fields Simultaneously, Phys. Rev. Appl. **13,** 064030 (2020).

[41] G. L. Dai, Y. H. Zhou, J. Wang, F. B. Yang, T. Qu, and J. P. Huang, Convective Cloak in Hele-Shaw Cells with Bilayer Structures: Hiding Objects from Heat and Fluid Motion Simultaneously, Phys. Rev. Appl. **17,** 044006 (2022).

[42] W.-S. Yeung and R.-J. Yang, *Introduction to Thermal Cloaking: Theory and Analysis in Conduction and Convection* (Springer, Singapore, 2022).

[43] J. X. Li, Y. Li, P.-C. Cao, T. Z. Yang, X.-F. Zhu, W. Y. Wang, and C.-W. Qiu, A continuously tunable solid-like convective thermal metadevice on the reciprocal line, Adv. Mater. **32,** 2003823 (2020).

[44] G. Q. Xu, K. C. Dong, Y. Li, H. G. Li, K. P. Liu, L. Q. Li, J. Q. Wu, and C.-W. Qiu, Tunable analog thermal material, Nat. Commun. **11,** 6028 (2020).

[45] N. P. Lu *et al.*, Electric-field control of tri-state phase transformation with a selective dual-ion switch, Nature **546,** 124 (2017).

[46] S. C. Deng, J. L. Yuan, Y. L. Lin, X. X. Yu, D. K. Ma, Y. W. Huang, R. C. Ji, G. Z. Zhang, and N. Yang, Electric-field-induced modulation of thermal conductivity in poly (vinylidene fluoride), Nano Energy **82,** 105749 (2021).

[47] J. Shin, J. Sung, M. Kang, X. Xie, B. Lee, K. M. Lee, T. J. White, C. Leal, N. R. Sottos, P. V. Braun, and D. G. Cahill, Light-triggered thermal conductivity switching in azobenzene polymers, Proc. Natl. Acad. Sci. U. S. A. **116,** 5973 (2019).

[48] J. M. Restrepo-Flórez and M. Maldovan, Mass diffusion cloaking and focusing with metamaterials, Appl. Phys. Lett. **111,** 071903 (2017).

[49] J. M. Restrepo-Flórez and M. Maldovan, Metamaterial membranes, J. Phys. D: Appl. Phys. **50,** 025104 (2017).

[50] L. Yang, C. B. Liu, Y. Bai, L. J. Qiao, and J. Zhou, Ultrathin hydrogen diffusion cloak, Adv. Theory Simul. **1,** 1700004 (2018).

[51] L. J. Xu, G. L. Dai, G. Wang, and J. P. Huang, Geometric phase and bilayer cloak in macroscopic particle-diffusion systems, Phys. Rev. E **102,** 032140 (2020).

[52] Z. R. Zhang and J. P. Huang, Transformation plasma physics, Chin. Phys. Lett **39,** 075201 (2022).

[53] F. Sun, Y. C. Liu, and S. L. He, Surface transformation multi-physics for controlling electromagnetic and acoustic waves simultaneously, Opt. Express **28,** 94 (2020).

[54] G. Y. Xing, W. X. Zhao, R. Hu, and X. B. Luo, Spatiotemporal modulation of thermal emission from thermal-hysteresis vanadium dioxide for multiplexing thermotronics functionalities, Chin. Phys. Lett. **38,** 124401 (2021).

[55] W. X. Zhao, Z. Zhu, Y. W. Fan, W. Xi, R. Hu, and X. B. Luo, Temporally-adjustable radiative thermal diode based on metal-insulator phase change, Int. J. Heat Mass Transf. **185,** 122443 (2022).

[56] See Supplemental Material at http://link.aps.org/supplemental/10.1103/PhysRevApplied.18.034080 for the dynamic evolution of parameters and physical fields.